J. of Electromagn. Waves and Appl., Vol. 21, No. 1, 57–70, 2007

ANALYSIS OF THE NONCONCENTRIC REFLECTOR ANTENNA-IN-RADOME SYSTEM BY THE ITERATIVE REFLECTOR ANTENNA AND RADOME INTERACTION

T. Oğuzer

Department of Electrical and Electronics Engineering
Dokuz Eylül University Tınaztepe Campus
35160 Buca İzmir, Turkey

A. Altintas

Department of Electrical and Electronics Engineering
Bilkent University
Bilkent Ankara, Turkey

Abstract—Nonconcentric reflector antenna-in-radome systems are used in applications especially requiring smaller radome coverages. The analysis of this two-dimensional geometry is performed for the E-polarization case. Here the geometry is decomposed into two parts and the analysis is performed by imposing the boundary conditions on each part as an iterative manner. This is known as the iterative boundary condition method in the literature. Convergence and accuracy are established numerically and it is seen that the expectations are really verified in reasonable CPU times. Also various numerical results are obtained for the description of the radiation characteristics.

1. INTRODUCTION

The radomes are frequently used to protect the reflector antennas from the environmental conditions. The accurate analysis of the radome covered reflector antenna system is an important topic especially for the engineering purposes. Even though in applications these systems exist in 3D, some 2D equivalents are also specifically of interest due to their nonvectorial nature. Sometimes 2D canonical scattering problems

can be solved with a rigorous analytical or numerical manner and they provide various valuable reference data.

One of the earliest methods to analyze the effect of the radome is the plane wave spectrum surface integration technique [1]. In that method, the aperture field distribution is considered as a bundle of rays which are traced through the radome wall. During this transmission the ray hitting the radome wall is assumed to be a local plane wave and the local geometry of the wall is taken as a planar slab. Later in the literature the ray tracing technique was improved by considering all possible ray combinations [2] and it is applied specifically to the circular cylindrical radome [3] by including considering the curvature effects into the solution. Also the radome covered 2D source radiation is analyzed by the modal cylindrical-wave spectrum instead of the plane wave spectrum [4] as a better approximation than the planar slab model. It can be said that in all these approaches the problem is considered as the radiation of a source through the radome wall and the multiple interactions between the source and the radome are ignored. In the above mentioned extended ray techniques some higher order rays are considered to model the whispering gallery modes inside the radome material. But, yet the interaction of the radome with an inner source like a reflector surface is still a complicated problem.

The radome problems can also be solved by using numerical methods like the method of moments [5] or the finite element techniques [6]. Even though these methods provide us the more accurate and smooth data than the hybrid ray techniques, they are mainly limited to the electrically small and medium size geometries.

In the radome covered antenna problems, the inclusion of the radome effect into the analysis is an essential point of the performed simulations. There exists some work in the literature to include the radome and antenna interactions into the analysis related with the method of moment procedure like given in [7]. Also in [8], for a hemispherical radome and a circular aperture type antenna, these interactions are considered by using the idea of reactional source variation which is implemented inside the analysis as an iterative manner and some mathematical expressions are obtained. This procedure in [8] provides one to solve larger geometries and the numerical results are obtained in reasonable CPU times.

Another important alternative in order to solve the similar reflector antenna and radome systems is the method of analytical regularization (MAR) [9]. It is a numerically rigorous method and one can classify it as a serious alternative when the high accuracy is desired in the numerical results. In this method the problem is formulated by considering the requirements of the presented boundary value problem

and therefore taking fully into account all interactions between the elements. The information about the radome is given in the kernel of the integral equation (IE) i.e., the Green's function obtained from the boundary conditions. To solve this rigorously defined IE by MAR, firstly it is converted into the discrete Fourier transform domain and then it is expressed in a dual series form. According to the semi-analytical procedure the most singular part of the kernel of original IE is extracted. Then this extracted part is inverted by Riemann-Hilbert problem (RHP) technique to perform analytical regularization. An algebraic matrix equation is obtained with the remaining part of the kernel but this time it is regularized matrix equation of the Fredholm 2nd kind. Therefore the convergence and accuracy can be achieved at a desired level.

A free space analysis of the 2D reflector antenna system was performed by combining the MAR technique with the complex source point (CSP) method in [10]. When the radome is considered the reflector surface and the radome may have the same axis i.e., the concentric one solved in [11] for both polarizations. The nonconcentric one which is widely used in practice especially for the small radome geometries was also analyzed by the combination of the MAR, Green's function and CSP methods in [12]. Then for the same problem the solution was tried to be improved by the usage of the available FFT algorithm in the computation of the Green's function in [13, 14]. By this way, larger geometries are simulated in reasonable CPU times.

Here an alternative solution is performed for the 2D circular reflector antenna-enclosed by a nonconcentrically located radome system. This solution is presented only for the E-polarization case. The idea of the procedure is based on the iterative boundary condition technique between the radome and the reflector surface. In an earlier paper [15], this method is applied to the scattering from two perfectly conducting circular cylinders. Then in [16], the similar iterative boundary condition technique is extended and used for the plane wave scattering from the arbitrarily oriented multi circular cylinders made up of the perfect conductor or dielectric materials. Also in [17], the Gaussian beam scattering from the similar circular cylinders are analyzed. In all these papers it is indicated that iterative boundary condition technique is very safe in terms of the convergence and accuracy. The solutions also are not restricted to the problem parameters. The presented reflector antenna-in-radome geometry can be assumed to be as a combination of the two parts. The first one is the reflector surface and its directive feed antenna. The radiation of this reflector antenna system can be found by using MAR following the procedure given in [9] and it is considered as an inner incident field

to the nonconcentric circular shell i.e., radome. Then this incident field is scattered inside by the radome shell causing secondary surface currents on the reflector surface. These secondary currents on the reflector surface again excites the shell resulting into iterative multiple scattering. The iteration scheme finally converges and provides us the total solution for the induced surface current density on the reflector surface and the far field radiation characteristics of the system can also be determined. Numerical results indicate that the precise results can be obtained in a few iteration number as shown by the relative error plots presented in the related section.

2. FORMULATION

The geometry of the reflector antenna and its covering radome system is given in Figure 1. In that figure, there is a 2D circular PEC reflector surface with radius a and half angle θ_{ap}. It is covered by a circular dielectric radome which is characterized by the relative permittivity ε_r and the relative permeability μ_r. Also the inner and outer radii of the radome are given as as c and d respectively. The center of the radome is shifted from the center of the reflector by a distance L. The feed is assumed to be a complex point line source and it radiates in the

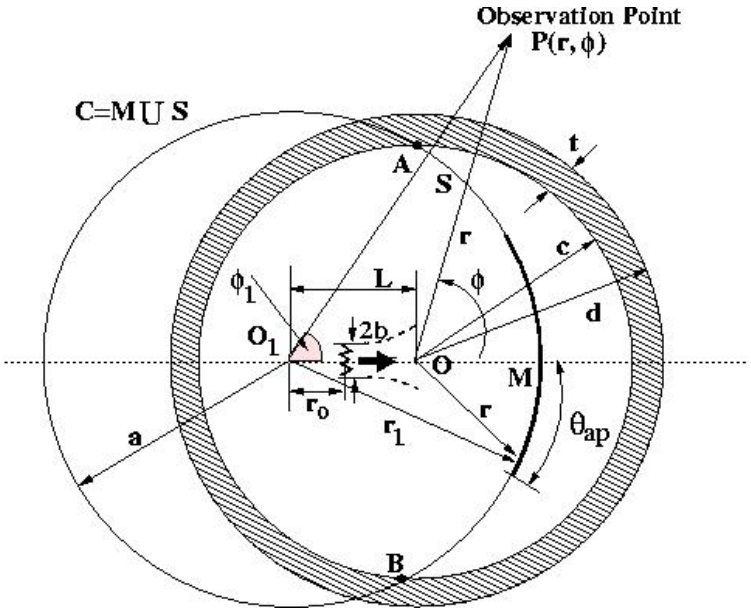

Figure 1. Geometry of the problem.

presence of the radome and the reflector surface. It is located on the symmetry axis of reflector-in-radome system preferably at $r_o = a/2$ point. The free space radiation from such a CSP line source having an electric type current is given by

$$E_z^{in}(\vec{r}) = H_0^{(1)}(k|\vec{r} - \vec{r}_s|) \tag{1}$$

where k is the free space wave number, $\vec{r}_s = \vec{r}_o + i\vec{b}$ is the complex source position, $\vec{r}_o$ is the real-space source position $\vec{b}$ and is the beam parameter vector. $\vec{r}_s$, $\vec{r}_o$ and $\vec{b}$ can be given in polar coordinates as $\vec{r}_s = (r_s, \varphi_s)$, $\vec{r}_o = (r_o, \varphi_o)$ and $\vec{b} = (b, \beta)$. Furthermore φ_o and β can be taken as zero for a symmetric feeding. Assuming that $\mathrm{Re}(r_s) > 0$ and $b > 0$ one finds that

$$r_s = \left[r_o^2 + i2r_o b\cos(\beta - \varphi_o) - b^2\right]^{1/2} \tag{2}$$

$$\varphi_s = \cos^{-1}\left((r_o\cos(\varphi_o) + ib\cos(\beta))/r_s\right) \tag{3}$$

The requirements of the problem can be stated as satisfying the 2-D Helmholtz wave equation, the Sommerfeld radiation condition at $r \to \infty$, the Meixner condition at the reflector edges, the Dirichlet boundary condition on the reflector surface M and further the tangential components of the electric and magnetic field have to be continuous on the radome boundaries.

The above requirements are crucial for the rigorous formulation of the presented problem. But here the solution will be performed by using an iterative boundary condition method and for this purpose, the geometry is separated into two parts. The first part is the reflector surface and the feed of the system. This means that the feed (complex source) radiates only in the presence of the reflector surface as for the definition of the first part. The solution of this problem can be found in terms of the Fourier series coefficients x_n's of the surface current density induced on the reflector by following the procedure defined in [9]. Then the radiated total electric field from this reflector antenna system can be written in the reflector based coordinate system (r_1, φ_1) as follows

$$E_{z,ref}^p(r_1, \varphi_1) = \sum_{n=-\infty}^{\infty} x_n^p \begin{pmatrix} J_n(ka)H_n^{(1)}(kr_1) & r_1 > a \\ J_n(kr_1)H_n^{(1)}(ka) & r_1 < a \end{pmatrix} e^{in\varphi_1} + \delta_{(p-1)0} H_0^{(1)}(k|\vec{r}_1 - \vec{r}_s|) \qquad p = 1, 2, \ldots \tag{4}$$

In the Equation (4), the second term in the right hand side presents the incident field and it can also be expressed as the Fourier series

form in the (r_1, φ_1) coordinate system. Also $\delta_{(p-1)0}$ is equal to 1 only when p is equal to 1 and zero else. The parameter p indicates the iteration number and so it is a natural number greater than zero i.e., $p = 1, 2, 3, \ldots$

The second part of the geometry is the circular shell i.e., the radome shell and it can be considered that the radome and the circular reflector surface are nonconcentric. Also the magnetic field component $H^p_{\varphi,ref}$ which is produced by the inner reflector antenna system can be found by using the Maxwell's equation of $H_\varphi = -\frac{1}{j\omega\mu}\frac{\partial E_z}{\partial r}$ in the radome centered coordinate system (r, φ). In this second iteration, the radome is excited by the radiated electric $(E^p_{z,ref})$ and the radiated magnetic $(H^p_{\varphi,ref})$ fields produced from the inner reflector antenna system. Then the additional scattered field is produced by the radome for the inner region i.e., $r < c$ when it is excited by $E^p_{z,ref}$ and $H^p_{\varphi,ref}$. But this time this inner scattered field by the radome will excite the reflector surface instead of the primary complex source feed.

To perform the above mentioned analysis, one has to be expand the $E^p_{z,ref}$ and $E^p_{\varphi,ref}$ into the Fourier series with respect to the radome centered (r, φ) coordinate system in the 0 to 2π region.

$$E^p_{z,ref}(r = c, \varphi) = \sum_{q=-\infty}^{\infty} e^p_{q,ref} e^{iq\varphi} \tag{5}$$

$$H^p_{\varphi,ref}(r = c, \varphi) = -\frac{k}{j\omega\mu} \sum_{q=-\infty}^{\infty} h^p_{q,ref} e^{iq\varphi} \tag{6}$$

where $e^p_{q,ref}$ and $h^p_{q,ref}$ are the corresponding Fourier series coefficients depending on the argument q. Also r_1 and φ_1 can be found in terms of φ and other problem parameters such as c and L by using the required geometrical transformation. Then these transformation formulas have to be used in the Equation (4) in order to obtain the Fourier series coefficients $e^p_{q,ref}$ and $h^p_{q,ref}$ existing in the Equations (5) and (6).

When the radome is excited from inside by the above defined electric and magnetic field components the following inner scattered field is produced by the radome [11]:

$$E^p_{z,rad} = \sum_{n=-\infty}^{\infty} A^p_n J_n(k_o r) e^{in\varphi} \qquad r < c \tag{7}$$

where $A^p_n = \frac{g_n c^p_n - f_n d^p_n}{g_n a_n - f_n b_n}$ and additionally a_n, b_n, c_n, d_n, f_n and g_n's are

given below.

$$a_n = J_n(kc)J_n'(k_oc) - \sqrt{\frac{\varepsilon_r}{\mu_r}}J_n(k_oc)J_n'(kc) \quad (8)$$

$$b_n = H_n^{(1)}(kc)J_n'(k_oc) - \sqrt{\frac{\varepsilon_r}{\mu_r}}J_n(k_oc)H_n^{(1)'}(kc) \quad (9)$$

$$c_n^p = h_{n,ref}^p J_n(kc) - \sqrt{\frac{\varepsilon_r}{\mu_r}}e_{n,ref}^p J_n'(kc) \quad (10)$$

$$d_n^p = h_{n,ref}^p H_n^{(1)}(kc) - \sqrt{\frac{\varepsilon_r}{\mu_r}}e_{n,ref}^p H_n^{(1)'}(kc) \quad (11)$$

$$f_n = J_n(kd)H_n^{(1)'}(k_od) - \sqrt{\frac{\varepsilon_r}{\mu_r}}J_n'(kd)H_n^{(1)}(k_od) \quad (12)$$

$$g_n = H_n^{(1)}(kd)H_n^{(1)'}(k_od) - \sqrt{\frac{\varepsilon_r}{\mu_r}}H_n^{(1)'}(kd)H_n^{(1)}(k_od) \quad (13)$$

By following the similar procedure given in [13, 14], the $E_{z,rad}^p$ in Equation (7) is directed to the reflector surface as a new incident field. It has to be evaluated on the whole $r_1 = a$ circle to proceed the iteration scheme. Therefore $E_{z,rad}^p$ is used as expressed in Equation (7) for the section inside the radome section and for the outside section i.e., $r > c$, the incident field can be approximated by a linear equation between the field values at the points $A(a, \varphi_m)$ and $B(a, 2\pi - \varphi_m)$. This new incident field can be written on the $r_1 = a$ circle as follows.

$$E_{z,rad}^{in}(r_1 = a, \varphi_1) = \sum_{n=-\infty}^{\infty} A_n^p g(r_1 = a, \varphi_1)e^{in\varphi} \quad (14)$$

where

$$g(r_1, \varphi_1, L) = \begin{cases} f(r_1, \varphi_1, L) & 0 \le \varphi_1 \le \varphi_m \text{ and } 2\pi - \varphi_m \le \varphi_1 \le 2\pi \\ \dfrac{\beta - \alpha}{2(\pi - \varphi_m)}\varphi_1 + \dfrac{\alpha(2\pi - \varphi_m) - \beta\varphi_m}{2(\pi - \varphi_m)} & \varphi_m < \varphi_1 < 2\pi - \varphi_m \end{cases} \quad (15)$$

and $\alpha = f(r_1, \varphi_m, L)$, $\beta = f(r_1, 2\pi - \varphi_m, L)$. The function f appearing in [15] is given as $f(r_1, \varphi_1, L) = J_n(k\sqrt{r_1^2 + L^2 - 2r_1L\cos\varphi_1})$. Also the appearing function f is given as $f(r_1, \varphi_1, L) = J_n(k\sqrt{r_1^2 + L^2 - 2r_1L\cos\varphi_1})$. Also φ is the function of the φ_1 and the other geometrical parameters like L and a. Then by using the inverse Fourier series method the required Fourier series coefficients b_n^p

can be found from the equation below.

$$E^{in}_{z,rad}(r_1 = a, \varphi_1) = \sum_{n=-\infty}^{\infty} b^p_n e^{in\varphi_1} \tag{16}$$

As a final step, one can conclude that the $E^{in}_{z,rad}$ gives inner scattered electric field correctly on the reflector surface depending on the previous current density coefficients x^p_n's. But this time it behaves as a new incident field and so the next iteration current density coefficients x^{p+1}_n's will be obtained. Then $E^{p+1}_{z,ref}$ can be written in the form of the Equation (4) but this time ignoring the field of the complex source feed.

The procedure defined above can be followed successively. This iterative boundary condition approach is used in literature and very strong convergence properties are observed [16, 17]. Here in the first part of the geometry dual series formulation is performed and then RHP based semi-analytical regularized solution is performed. The details of the method are given in [9]. For the second part of the geometry, the Fourier series based field expressions provides us the serial analytical solution. The iteration process goes between these two main solution procedures. Both methods for part 1 and part 2 of the problem show the good mathematical convergence and accuracy. Therefore one can expect the good convergence properties in the numerical results for the surface current density and far field radiation patterns for the whole system. The numerical results will be discussed in the next section.

3. NUMERICAL RESULTS

The presented formulation has been verified by computing the various relative truncation error plots, radiation patterns, and directivity. To generate all these results, we have used a PC notebook Pentium IV, 2.66 GHZ CPU and 256 MB RAM capacity with the windows 2000 operating system.

It is seen that the resultant equations have the convergent nature between two iterative solution techniques. However this statement has to be verified by the obtained numerical results. To verify the actual rate of convergence, we computed the relative error in the obtained surface current density and in the directivity. Here we imply these values in the sense of so-called maximum norm, i.e., $\Delta_x = \max\left|x^{N_{tr}+1}_n - x^{N_{tr}}_n\right| \Big/ \max\left|x^{N_{tr}}_n\right|$ and also the parameter demonstrating the error in the far field is defined as the relative accuracy in directivity

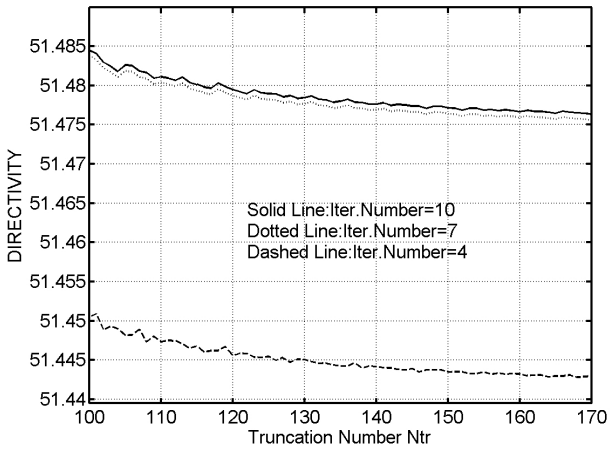

Figure 2. Directivity versus truncation number for different iteration numbers. The problem parameters are $ka = 62.83$, $kL = 50.26$, $kc = 94.24$, $\varepsilon_r = 2$, $\theta_{ap} = 30^\circ$, $kb = 2.6$ and $t = 0.4\lambda_e$.

i.e., $\Delta D = \left|D^{N_{tr}+1} - D^{N_{tr}}\right| \Big/ \left|D^{N_{tr}}\right|$. Here n is the Fourier series argument of the coefficient x_n till the final truncation number N_{tr}. Figure 2 shows that directivity versus truncation number variation for the different iteration numbers. It is seen that the directivity really converges with the increasing N_{tr} for each iteration number. Figure 3 presents the relative error in directivity and in the current density. Figure 3(a), 3(b) and 3(c) are plotted in logarithmic scale for different iteration numbers and it is observed that the relative error in the directivity and in the current density have the convergent behavior. The error in the directivity is lower than the surface current and this is an expected result defined in the theory.

Another important verification is the relative accuracy in directivity and the relative accuracy in the surface current density versus iteration number. For this purpose one has to define new maximum norms in terms of the iteration number q i.e., $\Delta_y = \max\left|x_n^{q+1} - x_n^q\right| \Big/ \max\left|x_n^q\right|$ for the relative error in the surface current density and $\Delta_y D = \left|D^{q+1} - D^q\right| \Big/ \left|D^q\right|$ for the relative error in the directivity. In these formulas N_{tr} is a pre-defined fixed value and maximum operation is taken with respect to the argument n. Depending on these formulas, Figure 4 presents the directivity and the relative error in the directivity and the surface current density.

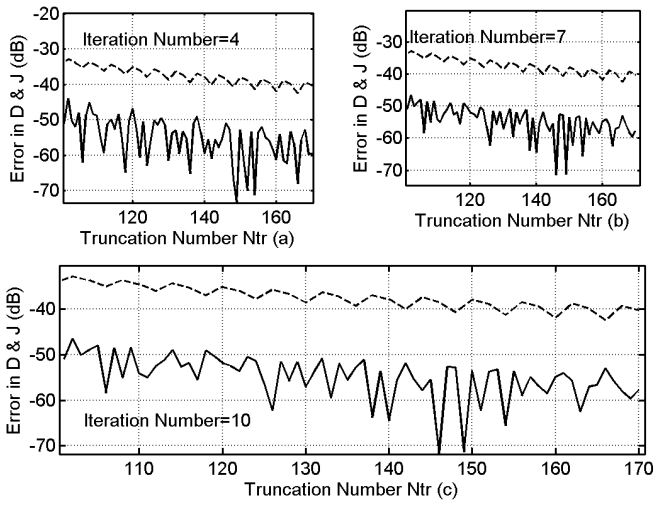

Figure 3. The relative error in directivity and in the surface current density in logarithmic scale versus the truncation number a) for the iteration number equals to 4 b) for the iteration number equals to 7 c) for the iteration number equals to 10. The solid line is the error in directivity and the dashed line is the error in the surface current density. The problem parameters are $ka = 62.83$, $kL = 50.26$, $kc = 94.24$, $\varepsilon_r = 2$, $\theta_{ap} = 30°$, $kb = 2.6$ and $t = 0.4\lambda_e$.

We have plotted in Figures 4(a) and 4(b) have plotted the above mentioned parameters in terms of the iteration number q for the different truncation numbers in logarithmic scale. The convergent behavior is also observed.

Figure 5 shows the normalized radiation pattern for the free space case and the different radome thicknesses. It yields almost the same radiation pattern as the free space case (no radome) and considerably reduces the pattern distortion which exists in the 0.4 f e radome thickness case.

Finally the Fourier series coefficients of the surface current density is plotted in terms of the numbers of the array for the different iteration numbers in the Figure 6(a). Even though five iteration is used, 3 iteration is enough for visible convergence as it is seen in Figure 6(a). Figure 6(b) shows the variation of the surface current density obtained from the present method and the solution given in [14]. The results are indistinguishable. To highlight the difference, in Figure 6(c), the surface current variation is compared with the similar result obtained

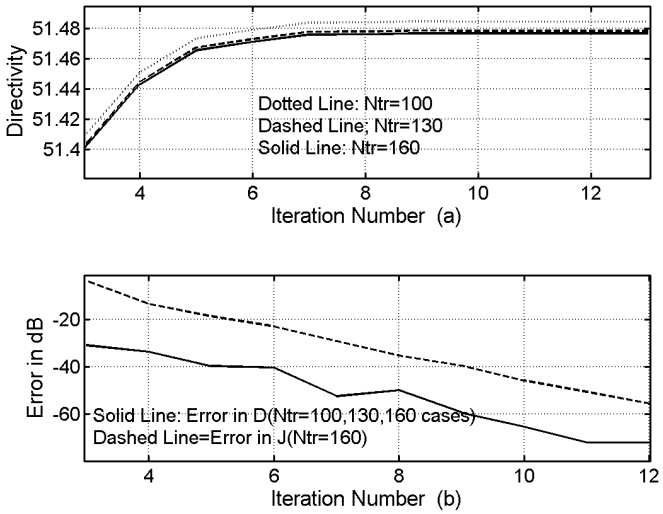

Figure 4. a) Directivity versus iteration number for the various truncation numbers. b) The relative error in the directivity and in the surface current density in logarithmic scale for the various truncation numbers. The problem parameters are $ka = 62.83$, $kL = 50.26$, $kc = 94.24$, $\varepsilon_r = 2$, $\theta_{ap} = 30^\circ$, $kb = 2.6$ and $t = 0.4\lambda_e$.

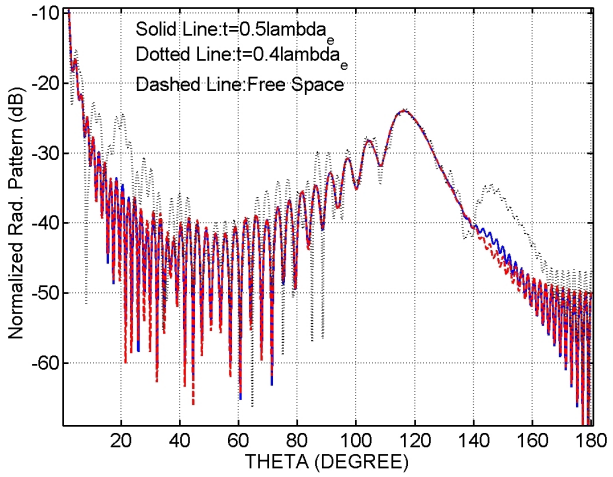

Figure 5. Normalized radiation pattern for the free space and for the different radome thicknesses ($\theta = \pi - \varphi$). The problem parameters are $ka = 157$, $kL = 125.6$, $kc = 175.84$, $kb = 2.6$, $\varepsilon_r = 2$, $\theta_{ap} = 30^\circ$.

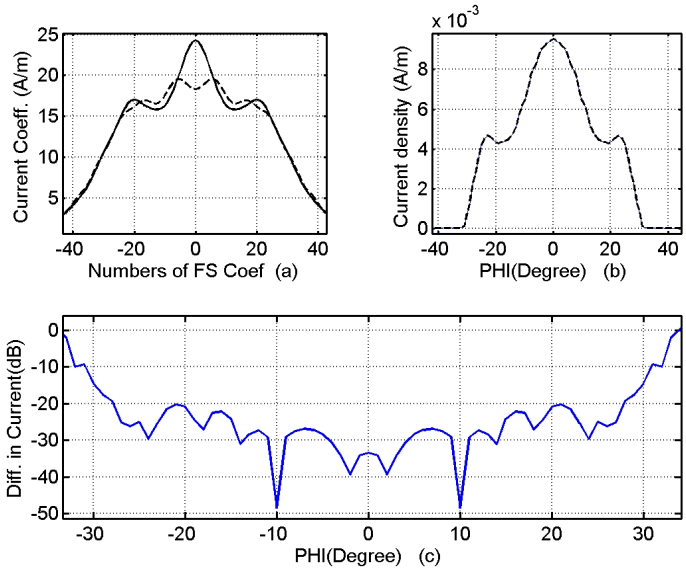

Figure 6. a) The Fourier series coefficients of the surface current density for the different iteration numbers (dashed line: iteration number is 1, dotted line: iteration number is 3, solid line: iteration number is 5). b) The surface current density variation over the reflector surface for the present and previous solutions. c) The relative difference between the present and the previous surface current densities over the reflector surface. The problem parameters are $ka = 94.24$, $kL = 75.39$, $kc = 113.09$, $kb = 2.6$, $t = 0.4\lambda_e$, $\varepsilon_r = 2$, $\theta_{ap} = 30^\circ$, Iteration number $= 9$.

in [14] and it is plotted as a relative error in the current i.e., the difference between two solution in the logarithmic scale. Except the near the edges, the relative error between two solution is less than the $-20\,\mathrm{dB}$ i.e., the two digit accuracy exist.

4. CONCLUSION

Two dimensional reflector antenna covered by a circular nonconcentric radome is analyzed by an iterative radome-antenna interaction procedure. The formulation presented is mathematically convergent and accurate as verified numerically. Also the radiation pattern for a larger geometry is presented and the written computer code works in reasonable CPU times.

ACKNOWLEDGMENT

The authors would like to thank Prof. Dr. Alexander I. Nosich for his useful suggestions and support.

REFERENCES

1. Wu, D. C. F. and R. C. Rudduck, "Plane wave spectrum surface integration technique analysis," *IEEE Trans. Antennas and Propagation,* Vol. AP-22, 497–500, May 1974.
2. Einziger, P. D. and L. B. Felsen, "Ray analysis of two-dimensional radomes," *IEEE Trans. Antennas and Propagation,* Vol. AP-31, No. 6, 870–884, November 1983.
3. Einziger, P. D. and L. B. Felsen, "Rigorous asymptotic analysis of transmission through a curved dielectric slab," *IEEE Trans. Antennas and Propagation,* Vol. AP-31, No. 6, 863–870, November 1983.
4. Chang, J.-H. and K.-K. Chan, "Analysis of a two-dimensional radome of arbitrarily curved surface," *IEEE Trans. Antennas and Propagation,* Vol. AP-38, No. 10, 165–1568, October 1990.
5. Arvas, E. and S. Ponnopalli, "Scattering cross section of a small radome of arbitrary shape," *IEEE Trans. Antennas and Propagation,* Vol. AP-37, May 1989.
6. Gordon, R. K. and R. Mittra, "Finite element analysis of axisymmetric radomes," *IEEE Trans. Antennas and Propagation,* Vol. AP-41, 975–980, 1993.
7. Li, L. W., I. Zhou, M. S. Leong, T, S. Yeo, and P. S. Kooi, "An open-ended circular waveguide with an infinite conducting flange covered by a dielectric hemispherical radome shell: Full-wave analysis and green dyadics," *Prog. Electromagn. Res.,* Vol. 21, 1998.
8. Li, L. W., M. S. Leong, L. Zhou, T. S. Yeo, and P. S. Kooi, "Improved analysis of antenna radiation from a circular aperture covered by a dielectric hemispherical radome shell," *IEE Proc. Microwave, Antennas Propag.,* Vol. 147, No. 2, April 2000.
9. Nosich, A. I., "MAR in the wave-scattering and eigenvalue problems: foundations and review of solutions," *IEEE Antennas Propagat. Magazine,* Vol. 42, No. 3, 34–49, 1999.
10. Oğuzer, T., A. Altintas, and A. I. Nosich, "Accurate simulation of reflector antennas by the complex source — dual series approach," *IEEE Trans. Antennas Propagat.,* Vol. AP-43, No. 8, 793–802, 1995.

11. Oğuzer, T., "Analysis of circular reflector antenna covered by concentric dielectric radome," *IEEE Trans. Antennas Propagat.,* Vol. AP-49, No. 3, 458–464, March 2001.
12. Yurchenko, V. B., A. Altintas, and A. I. Nosich, "Numerical optimization of a cylindrical reflector-in-radome antenna system," *IEEE Trans. Antennas Propagat.,* Vol. AP-47, No. 4 668–673, 1999.
13. Oğuzer, T., "Analysis of the 2D nonconcentric large reflector antenna-in-radome system: H-polarization case," *Mathematical Methods in Electromagnetic Theory International Symposium Proceedings,* Ukraine, September 2004.
14. Oğuzer, T. and A. Altintas, "Analysis of the nonconcentric radome-enclosed cylindrical reflector antenna system, E-polarization case," *Journal of Electromagnetic Waves and Applications,* Vol. 19, No. 15, 2093–2111, 2005.
15. Hongo, K., "Multiple scattering by two conducting circular cylinders," *IEEE Trans. Antennas and Propag.,* Vol. 26, No. 5, September 1978.
16. Elsherbeni, A. Z., "A comparative study of two-dimensional multiple scattering techniques," *Radio Science,* Vol. 29, No. 4, 1023–1033, 1994.
17. Elsherbeni, A. Z., M. Hamid, and G. Tian, "Iterative scattering of a gaussian beam by an array of circular conducting and dielectric cylinders," *Journal of Electromagnetic Waves and Applications,* Vol. 7, No. 10, 1323–1342, 1993.